

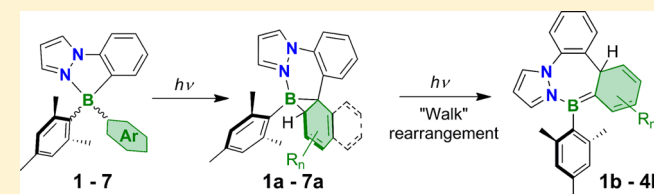
Accessing Two-Stage Regioselective Photoisomerization in Unsymmetrical N,C-Chelate Organoboron Compounds: Reactivity of B(ppz)(Mes)Ar

Cally Li, Soren K. Møllerup, Xiang Wang, and Suning Wang*

Department of Chemistry, Queen's University, Kingston, Ontario K7L 3N6, Canada

Supporting Information

ABSTRACT: A new family of unsymmetrical, N,C-chelate organoboron compounds B(ppz)(Mes)Ar have been synthesized and found to undergo a rare, regioselective two-stage photoisomerization, involving the Ar group only. The initial transformation is a Zimmerman rearrangement to afford yellow azaboratabisnorcaradiene isomers that are subsequently converted to unprecedented 14aH-diazaborepins via a photochemical “walk” rearrangement. Spectroscopic and computational studies provide insight into the formation and



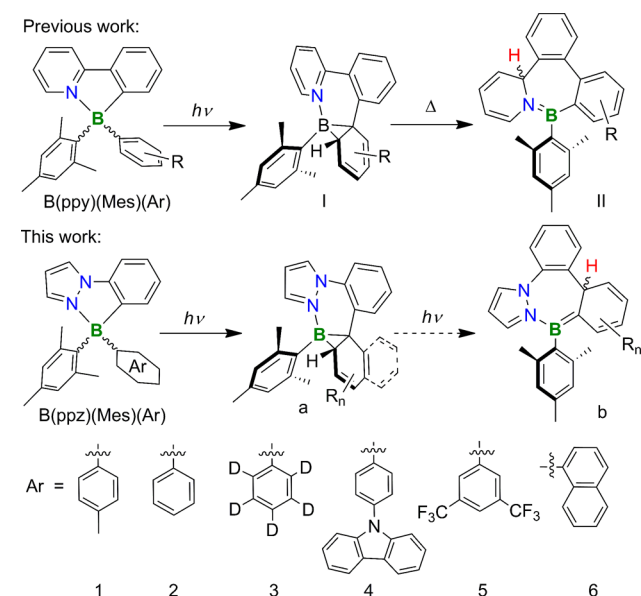
properties of these unique systems.

INTRODUCTION

Establishing the underlying mechanisms within chemical systems is important for both their practical implementation, as well as the discovery of new and useful processes/transformations. In this regard, the chemistry of organoboron compounds has received significant attention due to the rich optoelectronic properties of boron-doped π -systems¹ and their amenability toward numerous different fields in materials science such as chemical sensors,² organic light-emitting diodes (OLEDs),³ and memory devices.⁴ Our longstanding interest in photoresponsive boron compounds stems from the previously discovered N,C-chelate organoboron species B(ppy)(Mes)₂; ppy = 2-phenylpyridine, Mes = mesityl,⁵ which displays thermally reversible photochromic switching to generate a “dark” azaboratabisnorcaradiene isomer upon exposure to UV light. Following this initial discovery, many studies have since been devoted to examining the effects of altering the phenyl-pyridyl chelating backbone.⁶ It is only recently that our focus has shifted toward studying and understanding the influence of the aryl groups on boron, following the successful development of a one-pot approach for synthesizing various unsymmetrical derivatives bearing two different aryl substituents B(ppy)(Mes)Ar; Ar = ph or substituted ph; **Scheme 1**.⁷ While these unsymmetrical systems rely on the presence of one bulky Mes group to initiate the photoisomerization process, the formation of the borirane ring occurs regioselectivity on the less bulky Ar group (**I**; **Scheme 1**). Unlike their symmetric counterparts, these H-borirane dark isomers undergo a further thermal transformation into 4bH-azabor-epins (**II**; **Scheme 1**) by means of an H-atom migration from the borirane to the pyridyl moiety.⁷

In spite of this unique regioselective reactivity available to the unsymmetrical boron chelate compounds, their inability to thermally revert back to the original state means that these compounds are not photochromic, limiting their applicability

Scheme 1. Photochemical and Thermal Reactivity of B(ppy)(Mes)Ar/B(ppz)(Mes)Ar Compounds



in materials science. Given the propensity for the H atom in **I** to migrate to the electron deficient C2 position on the py ring, we postulated that photochromism may be achievable in these unsymmetrical derivatives if this kinetically favored pathway were blocked. We therefore designed a new series of chelate boron compounds (**1–7**), in which the electron deficient C2 position of py has been replaced by an electron-rich nitrogen atom of pyrazole (pz). Although **1–7** undergo the expected

Received: August 18, 2018

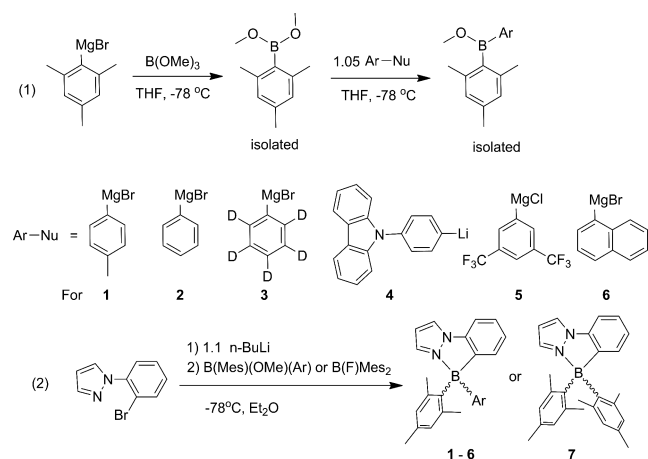
regioselective photoisomerization into their respective azaboratabisnorcaradienes (**a**), the resulting isomers are all thermally inert. In lieu of this, prolonged irradiation of certain derivatives facilitated their conversion into unprecedented 14a*H*-diazaborpins or BNN-benzotropolidene (e.g., **1b–4b**). Although the B(ppz)(Mes)Ar (ppz = 1-phenylpyrazole) compounds do not possess the anticipated reversible photochromism, their two-stage photoreactivity indicates that this type of rare isomerism^{6a} is a general phenomenon for N,C-chelate organoborates with diazole donors.

RESULTS AND DISCUSSION

Syntheses and Structures of Compounds 1–7.

Compounds **1–7** were prepared in low to moderate yields via a one-step lithiation of 1-(2-bromo-phenyl)-1*H*-pyrazole, followed by the addition of the appropriate B(Mes)(OMe)(Ar) reagent or B(F)Mes₂ (Scheme 2). B(Mes)(OMe)(Ar)

Scheme 2. Synthesis of B(ppz)(Mes)(Ar) and B(ppz)Mes₂



reagents were prepared using modified literature procedures,⁷ which involves the addition of 1.05 equiv of the corresponding Grignard/lithiated reagent (Ar–Nu; Scheme 2) to B(Mes)(OMe)₂ (see Experimental Section and Supporting Information (SI) for details). All compounds were fully characterized by ¹H, ¹³C, ¹¹B NMR and HRMS spectroscopic methods.

The crystal structures of **4** and **6** were determined by single-crystal X-ray diffraction analysis (see the Supporting Information) and are shown in Figure 1. Unsurprisingly, the steric congestion imposed by the bulky Mes group induces B–CAr/Mes bonds of 1.62–1.64 Å, which is a feature known to be essential for instigating photoisomerization.^{7,8} The B–N

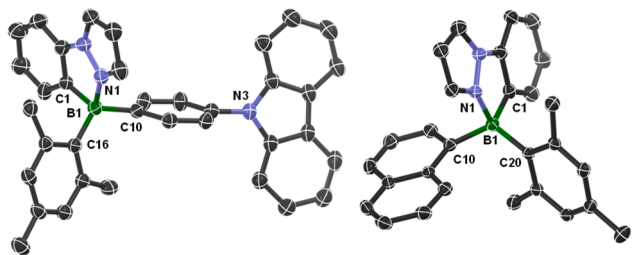


Figure 1. Crystal structures of **4** (left) and **6** (right). Selected bond lengths (Å) for **4**: B1–C1 1.611(5), B1–N1 1.630(5), B1–C10 1.621(5), B1–C16 1.627(5); for **6**: B1–C1 1.618(4), B1–N1 1.648(3), B1–C10 1.638(4), B1–C20 1.626(4).

bond lengths in these two molecules are 1.630(5) and 1.648(3) Å, respectively, similar to those with ppz and derivatives as the chelate units.⁶ In compound **4**, the carbazole ring and the phenyl ring are not coplanar with a dihedral angle of 73.3(2)°.

Photophysical Properties of Compounds 1–7. The absorption spectra and fluorescence spectra of **1–7** are shown in Figure 2, and the data are summarized in Table 1.

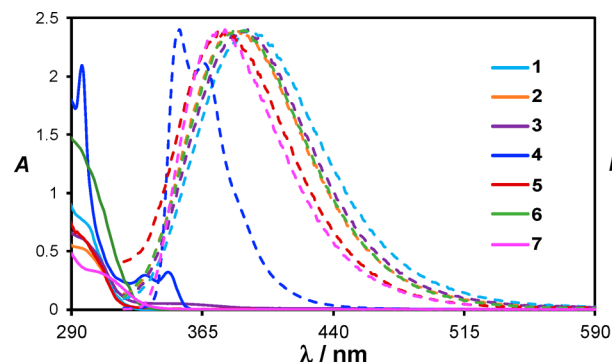


Figure 2. UV/vis and normalized fluorescence (dashed lines) spectra of **1–7** in toluene at 10^{−4} M.

Table 1. Photophysical Properties of Compounds **1–7**

compd	λ_{abs} (nm) (ϵ , M ^{−1} cm ^{−1}) ^a	λ_{em} (nm)	Φ_{fl}
1	300 (7.11 × 10 ³)	392	0.19
2	298 (5.11 × 10 ³)	384	0.11
3	296 (6.10 × 10 ³)	391	0.08
4	296, 333, 347 (2.10 × 10 ⁴ 104)	352, 368	0.33
5	294 (6.53 × 10 ³)	374	0.10
6	297 (1.33 × 10 ⁴)	383	0.12
7	305 (3.22 × 10 ³)	398	0.12

^a10^{−4} M in toluene at 298 K

Compounds **1–7** have intense absorption in the mid-UV region, with $\lambda_{\text{abs}} < 300$ nm in all cases except **4**. Compared to previously reported N,C-chelate organoborates, these values are similar to those observed for systems with *N*-heterocyclic carbene (NHC) donors^{6c} and hypsochromically shifted by ~60 nm relative to species with pyridine as the donor.^{5,7,8} This is due to HOMO stabilization induced by the electron-accepting ability of pyrazole. TD-DFT calculation data (at the cam-B3LYP¹⁵/SVP¹⁶ level of theory; see the Supporting Information) indicate that the primary absorption bands of **1–2** and **4–7** have different contributions depending on the substituent. Compounds **1**, **6**, and **7** have an S₁ transition that corresponds to a HOMO (π -Mes/Ar) → LUMO (π^* -ppz) charge transfer (CT), which is characteristic of these systems.^{6–8} Conversely, **2** and **5** possess HOMO-2 → LUMO as the main contribution to their S₁, where HOMO-2 is delocalized across both the aryl substituents and ppz backbone. The predicted S₁ transition for compound **4** has HOMO → LUMO+1 as its primary contributor, which is a π → π^* transition centered on the carbazole unit. This is in agreement with experimental data, as compound **4** is the only species to have well resolved vibrational features in its absorption spectra, which are a combination of S₁ and S₂ (CT transitions; HOMO → LUMO, 38%; HOMO-4 → LUMO, 46%; see SI). The fluorescence spectra of **1–7** exhibit a hypsochromic shift relative to the related N,C-chelate boron

analogues,^{5,7,8} such as B(ppy)(Mes)Ar with $\lambda_{em} = 360\text{--}390$ nm and relatively low quantum yields ($\Phi_f = 0.10\text{--}0.33$). In contrast to the broad featureless CT emission bands of the other five compounds, compound **4** exhibits a structured emission spectrum which is most hypsochromically shifted and has the highest Φ_f (0.33), attributable to the carbazole unit.⁹

Photoisomerization. The response of compound **1** toward UV light was examined first. Upon irradiation at 300 nm in C_6D_6 , **1** undergoes two-stage sequential color changes: colorless to yellow, then to deep-orange (Figure 3).

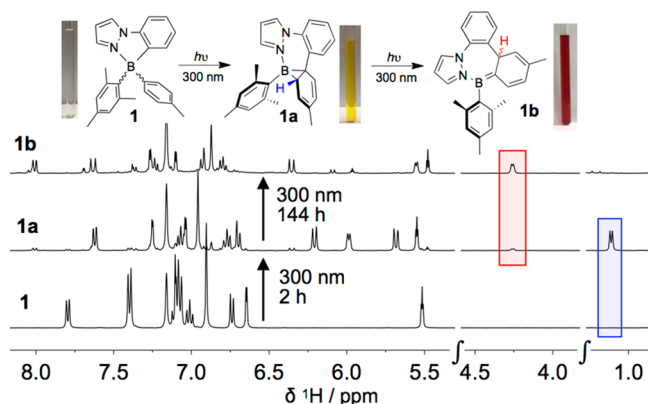


Figure 3. Partial 1H NMR spectra in C_6D_6 showing the conversion of **1** \rightarrow **1a** \rightarrow **1b** with diagnostic chemical shifts highlighted in blue (**1a**) and red (**1b**). Inset: photographs showing the solution colors of the three different species at 10^{-2} M in benzene.

Monitoring the reaction by NMR spectroscopy revealed the initial transformation of **1** into its dark borirane isomer **1a**, as evidenced by diagnostic 1H and ^{11}B chemical shifts at $\delta \approx 1.11$ (H atom on borirane; $^3J = 6.1$ Hz) and -15 ppm, respectively. From 2D NMR data, it is clear that **1** goes through the same regioselective photoisomerization as the B(ppy)(Mes)(Ar) molecules,⁷ in which the borirane forms exclusively on the less bulky tolyl group. The formation of **1a** and its characteristic yellow color is further corroborated by UV/vis spectroscopy, as the gradual irradiation of **1** causes a steady growth of a new low energy absorption band at $\lambda_{abs} \approx 439$ nm (Figure 4 and SI). Akin to what has been observed for **I** in Scheme 1, this broad band emerging in the visible region is a result of a CT transition from HOMO (σ -borirane + π -cyclohexadienyl ring) to LUMO (π^* -ppz). Extended irradiation for several hours leads to a second stage color change from yellow to orange, as the 1H and ^{11}B peaks of **1a** vanish in the NMR spectra, and a

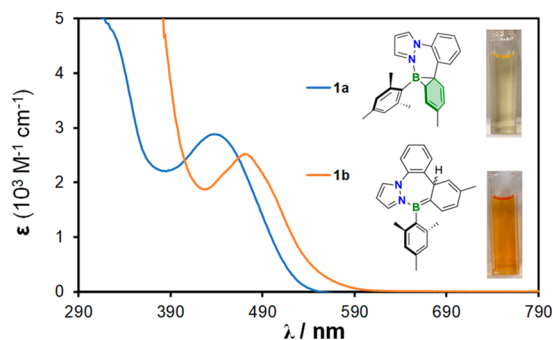


Figure 4. UV/vis absorption spectra of **1a** and **1b** in toluene. Inset: photographs showing their colors in solution.

new set of peaks belonging to **1b** appear. The structure of **1b** was characterized by comprehensive 1D and 2D NMR analysis (Figure 5 and SI). The $^1H\text{--}^1H$ COSY spectrum shows

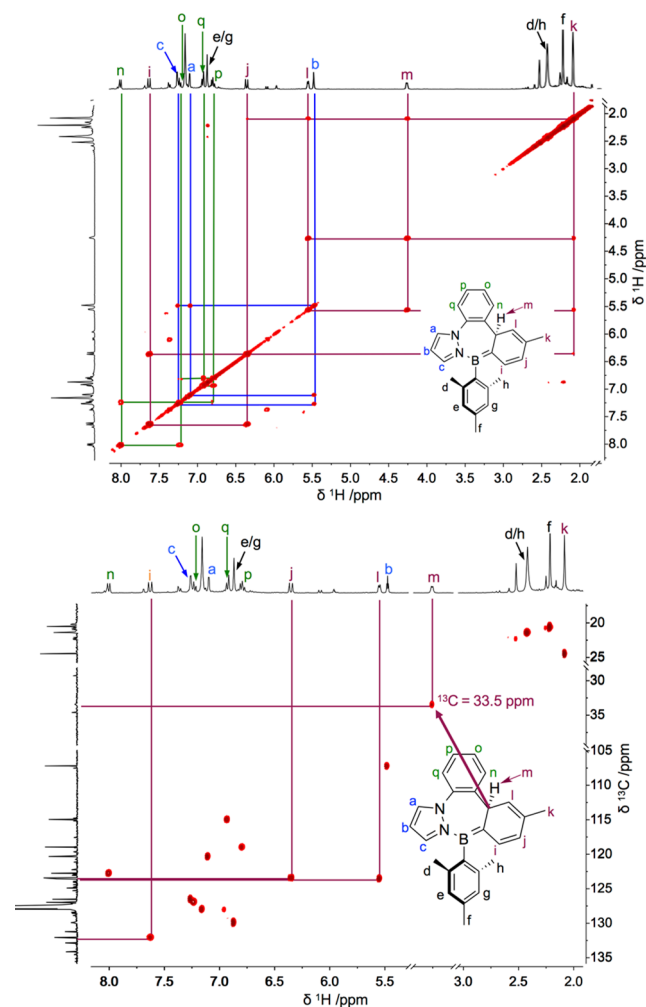


Figure 5. $^1H\text{--}^1H$ COSY spectrum (top) and $^1H\text{--}^{13}C$ HSQC spectrum (bottom) of **1b** in C_6D_6 with diagnostic correlations.

correlations between the three olefin protons and a CH_3 group (tolyl), indicating the preservation of a cyclohexadiene bonding arrangement. More noteworthy is the coupling of one olefin proton to the upfield-shifted H atom ($\delta \approx 4.26$ ppm, $^3J = 4.7$ Hz; doublet) on the same ring, which, according to $^1H\text{--}^{13}C$ HSQC data, is attached to a quaternary carbon center ($\delta^{13}C \approx 33.5$ ppm). A new ^{11}B resonance at ~ 29 ppm is observed, comparable to the chemical shift values of previously reported $R_2B=C(R')(R'')$ systems¹⁰ and the closely related 1,2-azaborabenzotripyridene (BN-BTPD) molecule^{6a} (Figure 6). All of these data led us to ascribe a similar seven-membered BNN-BTPD structure for **1b**. Due to the structural similarities between BN-BTPD and **1b**, a similar two-stage photochemical reaction pathway via “walk” rearrangement established previously for BN-BTPD formed from photoisomerization of B(Me-imidazolyl-ph)Mes₂ is likely responsible for the formation of **1b**. The key difference between BN-BTPD and **1b** is that the former can thermally revert back to its parent chelate species, whereas **1b** is thermally inactive. Hence, it should be noted that the thermally accessible, ground-state “walk” rearrangement observed for BN-BTPD and its

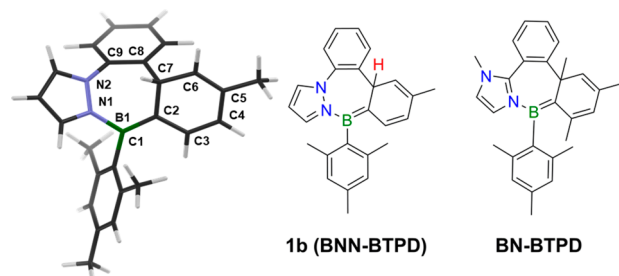


Figure 6. Diagrams showing the structures of **1b** and BN-BTPD (right) and the DFT-optimized structure of **1b** (left) obtained with the cam-B3LYP/SVP level of theory. Key bond lengths (Å) for **1b**: B1–C1 1.584, B1–C2 1.455, B1–N1 1.543, N1–N2 1.357, N2–C9 1.434, C2–C7 1.533, C2–C3 1.411, C3–C4 1.354, C4–C5 1.461, C5–C6 1.344, C6–C7 1.509, C7–C8 1.520, C8–C9 1.400.

respective isomers cannot be applied to the molecules in this study.

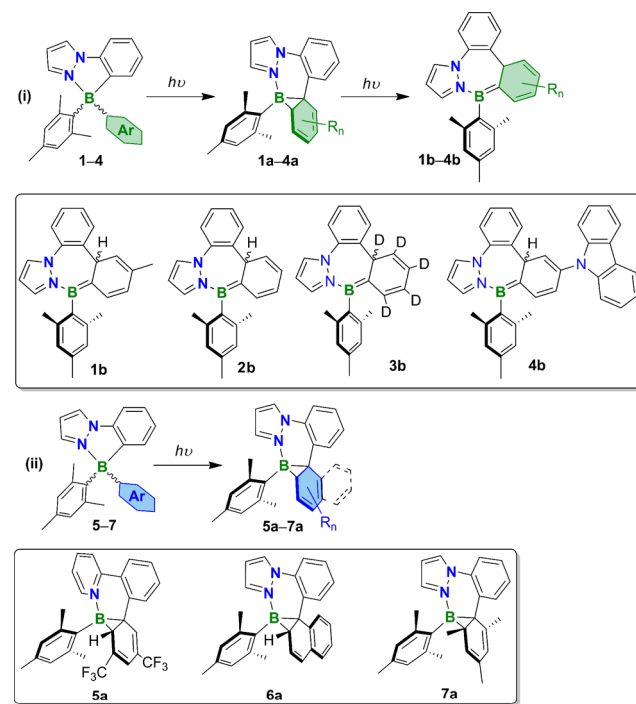
Upon exposure to air, **1b** decomposes rapidly, a common feature of molecules bearing a B=C bond.¹⁰ Unfortunately, attempts to obtain single crystals of **1b** for X-ray diffraction analysis were unsuccessful due to the formation of a small amount of unknown side product during the generation of **1b** and the highly air-sensitive nature of **1b**. Insight into the structural configuration of **1b** is gained by its DFT-optimized structure shown in Figure 6. The calculated B=C bond length of 1.45 Å is comparable to that of the BN-BTPD system (1.47 Å) and to values reported for [Mes₂B=CH₂]^{−10c} as well as Lewis acidic methyleneboranes.¹¹ Accompanying the conversion of **1a** → **1b** is a color change from yellow to orange, which corresponds to an ~40 nm bathochromic shift in the absorption band of **1b** relative to that of **1a** (Figure 4). According to TD-DFT calculations, the HOMO of **1b** is localized on the conjugated B=C bond and the cyclohexadienyl moiety while the LUMO is localized on the ppz unit. On the basis of what has been observed for BN-BTPD, the destabilized HOMO orbital of **1b** compared to that of **1a** is likely responsible for its increased λ_{abs} value. From TD-DFT data, the primary absorption band of **1b** was assigned to a HOMO → LUMO CT transition. The calculated and experimental UV/vis spectra of **1b** match very well, further validating the formation of the proposed structure for **1b** (see the Supporting Information).

In light of the interesting reactivity of **1**, the influence of electronic effects on the two-stage photoisomerization process was examined by substituting the boron center with various aryl groups. As evidenced by their NMR and UV/vis spectra (see the Supporting Information), compounds **2–6** undergo the initial regioselective photoisomerization into their respective borirane isomer “a”. Irradiation at 300 nm induces the growth of a broad CT (HOMO → LUMO) absorption band between 370 and 440 nm for all compounds, giving a pale-yellow color to each of the dark isomers. Given that the LUMO of the borirane in all cases is composed of the π* orbitals on the ppz chelate, the difference in absorption λ_{max} must be dictated by the substituents undergoing photoisomerization.

Notably, the λ_{abs} values of **5a** and **6a** are hypsochromically shifted (~30 to 60 nm) relative to those of **1a–4a**, signifying a stabilization of their HOMO orbitals, which is likely a result of the electron-withdrawing properties of the 3,5-(CF₃)₂C₆H₃ substituent in **5a** and the extended π-conjugation of the

naphthyl ring in **6a**. Continued irradiation causes **2a** and **3a** to undergo the same isomerism as **1a**, although their final ¹H NMR spectra reveal a mixture of products comprising the corresponding isomer **2b/3b**, analogues of **1b**, and a minor unidentifiable species **2b’/3b’** (see Scheme 3 and the

Scheme 3. Summary of Photochemical Reactivity of B(ppz)(Mes)(Ar) Compounds



Supporting Information). Due to the overlapping NMR signals and the instability of the minor products, **2b’** and **3b’** could not be fully characterized. The five ¹H resonances of the cyclohexadienyl protons in **2b** are absent in the ¹H NMR spectrum of **3b** (see the Supporting Information), further confirming the assignment of the BNN-BTPD structure. The isomerization of **4a** → **4b** was also observed, albeit it proceeds with the formation of minor degradation products. Correspondingly, the characteristic orange colors of **2b–4b** are consistent with their red-shifted absorption bands emerging between 470–510 nm.

Interestingly, extended irradiation of **5a** and **6a** results in no spectral change according to ¹H and ¹¹B NMR spectral data, confirming that their “b” isomers are not formed. The lack of photoreactivity of **5a** is attributable to the CF₃ groups, which stabilizes the HOMO orbital of the molecule (borirane/cyclohexadienyl). This stabilized HOMO level prevents any further photochemical transformations that would otherwise occur through the excited state. In the case of **6a**, the increased steric bulk imposed by the naphthyl substituent is likely restricting further intramolecular bond rearrangement around the boron center. Although having one Mes group in these systems is crucial for instigating photoisomerization, it seems that excessive crowding by two bulky aryl groups is not conducive to transformations beyond the dark isomer. For example, the symmetric derivative B(ppz)(Mes)₂ (compound **7**, Scheme 3) was synthesized in an effort to probe the full range of photoreactivity in this series of molecules. When irradiated at 300 nm, B(ppz)(Mes)₂ mirrors the reactivity of **6**

and is only able to undergo one-step isomerization into its dark isomer (**7a**). To the same extent, the steric congestion inflicted by bulky *o*-CH₃ groups on Mes renders a restricted conformation around boron, such that further isomerization of the dark isomer is not feasible. Compared to the dark isomer formed from B(Me-imidazolyl-*ph*)Mes₂, **7a** is clearly stable toward “walk” rearrangement to form **7b**. These findings suggest that the nature of the chelate backbone has a great impact on the photoisomerization pathways, and furthermore, the photochemical generation of the azabora-BTPD molecules not only favors the more electron-rich substituent, but also requires controlled steric bulk around the B atom.

CONCLUSIONS

In summary, six new unsymmetrical organoboron molecules have been prepared and studied. All compounds are photoresponsive and undergo regioselective isomerization into their respective azaboratabisnorcaradiene isomers. With suitable functionalization and steric control around the boron center, these species can further transform into rare 14*a*H-diazabor-epins/BN-tropilidenes. This two-stage photoisomerization is mechanistically similar to that of our previously reported *N*-methyl-2-phenylimidazolyl-chelated B(Mes)₂ systems, as implicated by the structural and photophysical resemblances observed between the diazaborepins and BN-BTPD. Nevertheless, this work marks the first of such a reaction pathway observed for chiral N,C-chelate organoboron compounds and illustrates the diverse range of excited-state pathways that can be accessed by altering their electronic structure.

EXPERIMENTAL SECTION

General Methods and Procedures. All experiments were carried out under an inert atmosphere of N₂ using standard Schlenk techniques. All starting materials were purchased from Sigma-Aldrich and used without further purification. 1-(2-Bromophenyl)-1*H*-pyrazole,¹² 9-(4-bromophenyl)-9*H*-carbazole,¹³ and B(OMe)₂(Mes)^{7b} were prepared according to literature procedures. All solvents were dried over Na and degassed. ¹H, ¹¹B, and ¹³C NMR spectra were recorded on a Bruker Avance 400, 600, or 700 MHz spectrometer. Deuterated solvents were purchased from Cambridge Isotopes and dried/degassed prior to use. Photochemical reactions were performed in J-Young NMR tubes and photochemical reactions were carried out using a Rayonet Photochemical Reactor. High resolution mass spectra (HRMS) were obtained using a Micromass GCT TOF-EI mass spectrometer. Excitation and emission spectra were recorded using a Photon Technologies International Quanta-Master Model 2 spectrometer. UV-visible spectra were recorded on a Varian Cary 50 spectrometer. Photoluminescent quantum yields were measured using a Hamamatsu QY spectrometer (C11347-11). The purity of compounds **1**–**7** was established by ¹H and ¹³C NMR spectroscopic analyses.

DFT/TD-DFT Calculation Details. DFT and TD-DFT calculations were performed using the Gaussian 09 suite of programs¹⁴ on the High Performance Computing Virtual Laboratory (HPCVL) at Queen's University. Geometry optimizations and vertical excitations of all compounds were obtained at the cam-B3LYP¹⁵/SVP¹⁶ level of theory, with the resulting structures confirmed to be stationary points through vibrational frequency analysis.

Synthesis of 1. In a 50 mL oven-dried Schlenk flask, *p*-tolylmagnesium bromide was prepared from 4-bromotoluene (0.856 g, 5 mmol), magnesium turnings (0.221 g, 5 mmol), and a small iodine crystal in THF (15 mL). The mixture was refluxed for 2 h at 80 °C until all the magnesium disappeared and then slowly cooled to –78 °C using a dry ice/acetone bath. After 30 min of cooling, the flask was charged with B(OMe)₂(Mes) (0.914 g, 4.76 mmol) and the resulting B(OMe)(Mes)(*p*-tolyl) solution was warmed to ambient

temperature overnight. The solvent was removed *in vacuo*, and the residue was extracted with dry/degassed hexanes (200 mL). The crude mixture was filtered through Celite under N₂ and concentrated under reduced pressure. A separate 50 mL Schlenk was charged with 1-(2-bromophenyl)-1*H*-pyrazole (0.736 g, 3.3 mmol) and Et₂O (15 mL). The solution was cooled to –78 °C for 30 min, after which *n*-BuLi (1.5 mL, 3.63 mmol, 2.5 M in hexanes) was added dropwise. After the lithiated ligand solution was allowed to stir for 1 h at –78 °C, B(OMe)(Mes)(*p*-tolyl) was added quickly and the completed reaction mixture was slowly warmed to ambient temperature overnight. The solvents were removed under reduced pressure, and the crude product was purified with flash column chromatography using a gradient elution (10:1 → 4:1 hexanes:ethyl acetate). **1** was obtained as a white solid in 45% yield (0.31 g). ¹H NMR (400 MHz, C₆D₆): δ 7.79 (d, *J* = 7.2 Hz, 1H, Ph–H), 7.40 (d, *J* = 7.7 Hz, 2H, *p*-tolyl–H), 7.13–7.05 (m, 4H, Pz–H, *p*-tolyl–H, and Ph–H), 7.01 (t, *J* = 7.3 Hz, 1H, Ph–H), 6.90 (s, 2H, Mes–H), 6.74 (d, *J* = 7.8 Hz, 1H, Ph–H), 6.65 (d, *J* = 2.5 Hz, 1H, Pz–H), 5.52 (t, *J* = 2.4 Hz, 1H, Pz–H), 2.28 (s, 3H, *p*-Mes–CH₃), 2.18 (s, 3H, *p*-tolyl–CH₃), 1.94 (s, 6H, *o*-Mes–CH₃) ppm; ¹³C NMR (100 MHz, C₆D₆) δ 142.5, 138.3, 134.7, 134.4, 133.6, 132.7, 132.1, 130.1, 129.0, 125.9, 121.3, 110.2, 109.5, 25.3, 21.3, 20.9 ppm; ¹¹B NMR (128 MHz, C₆D₆) δ 1.8 ppm; HRMS (EI), calcd for C₂₅H₂₅BN₂ [M]⁺: 364.2111, found 364.2101.

Synthesis of 2. Compound **2** was synthesized using the same procedure as that for compound **1**, where bromobenzene was used to prepare the second Grignard reagent in the synthesis of B(OMe)(Mes)(Ph). **2** was obtained as a white powder in 30% yield (0.21 g). ¹H NMR (400 MHz, C₆D₆): δ 7.77 (dd, *J* = 7.2, 1.3 Hz, 1H, Ph–H), 7.46 (m, 2H, B–Ph–H), 7.21 (dd, *J* = 8.0, 6.7 Hz, 2H, B–Ph–H), 7.14–7.08 (m, 2H, Ph–H and B–Ph–H), 7.07 (d, *J* = 2.4 Hz, 1H, Pz–H), 7.00 (td, *J* = 7.6, 1.3 Hz, 1H, Ph–H), 6.89 (s, 2H, Mes–H), 6.73 (d, *J* = 7.8 Hz, 1H, Ph–H), 6.62 (d, *J* = 2.6 Hz, 1H, Pz–H), 5.49 (t, *J* = 2.5 Hz, 1H, Pz–H), 2.27 (s, 3H, *p*-Mes–CH₃), 1.91 (s, 6H, *o*-Mes–CH₃) ppm; ¹³C NMR (100 MHz, C₆D₆) δ 142.55, 138.3, 134.8, 133.6, 133.3, 132.7, 132.1, 130.1, 125.9, 125.62, 121.4, 110.3, 109.6, 25.3, 20.9 ppm; ¹¹B NMR (128 MHz, C₆D₆) δ 1.6 ppm; HRMS (EI), calcd for C₂₄H₂₃BN₂ [M]⁺: 350.1954, found 350.1969.

Synthesis of 3. Compound **3** was synthesized using the same procedure as that for compound **1**, where bromobenzene-*d*₅ was used to prepare the corresponding Grignard and B(OMe)(Mes)(Ph) reagents. **3** was obtained as an orange solid in 19% yield (0.07 g). ¹H NMR (400 MHz, C₆D₆): δ (d, *J* = 7.2 Hz, 1H, Ph–H), 7.10 (t, *J* = 7.3 Hz, 1H, Ph–H), 7.07 (d, *J* = 2.5 Hz, 1H, Pz–H), 7.01 (td, *J* = 7.5, 1.1 Hz, 1H, Ph–H), 6.89 (s, 2H, Mes–H), 6.73 (d, *J* = 7.8 Hz, 1H, Ph–H), 6.63 (d, *J* = 2.7 Hz, 1H, Pz–H), 5.50 (t, *J* = 2.5 Hz, 1H, Pz–H), 2.27 (s, 3H, *p*-Mes–CH₃), 1.91 (s, 6H, *o*-Mes–CH₃) ppm; ¹³C NMR (100 MHz, C₆D₆) δ 142.5, 138.3, 134.8, 133.6, 132.7, 130.1, 128.3, 128.0, 127.8, 127.3, 125.9, 121.3, 110.3, 109.6, 25.31, 20.9 ppm; ¹¹B NMR (128 MHz, C₆D₆) δ 1.6 ppm; HRMS (EI), calcd for C₂₄H₁₈D₅BN₂ [M]⁺: 355.2268, found 355.2265.

Synthesis of 4. Compound **4** was synthesized using a similar procedure as that for compound **1**. To prepare the (4-(9*H*-carbazol-9-yl)phenyl)lithium solution, 9-(4-bromophenyl)-9*H*-carbazole (1.61 g, 5 mmol) was dissolved in THF (~15 mL) and cooled to –78 °C using a dry ice/acetone bath. After 30 min, *n*-BuLi (2.3 mL, 5.8 mmol, 2.5 M in hexanes) was added dropwise and the mixture was stirred for 1 h to afford the lithiated reagent. The lithiated solution was used as is in the next step to prepare B(OMe)(Mes)(*p*-Ph–Cbz), following the same procedures described above. **4** was obtained as an off-white powder in 34% yield (0.30 g). ¹H NMR (400 MHz, C₆D₆): δ 8.07 (d, *J* = 7.5 Hz, 2H, Cbz–H), 7.79 (d, *J* = 7.3 Hz, 1H, Ph–H), 7.52 (d, *J* = 7.9 Hz, 2H, Cbz–H), 7.37 (d, *J* = 8.0 Hz, 2H, B–Ph–H), 7.31–7.18 (m, 6H, B–Ph–H and Cbz–H), 7.13 (m, 2H, Ph–H and Pz–H), 7.09 (d, *J* = 2.4 Hz, 1H, Pz–H), 7.03 (t, *J* = 7.5 Hz, 1H, Ph–H), 6.94 (s, 1H, Mes–H), 6.77 (d, *J* = 7.8 Hz, 1H, Ph–H), 6.68 (d, *J* = 2.7 Hz, 1H, Pz–H), 5.57 (t, *J* = 2.6 Hz, 1H, Pz–H), 2.29 (s, 3H, *p*-Mes–CH₃), 1.93 (s, 6H, *o*-Mes–CH₃) ppm; ¹³C NMR (100 MHz, C₆D₆) δ 142.6, 141.9, 133.7, 133.4, 132.7, 130.26, 128.3, 128.0, 127.8, 127.5, 126.2, 126.1, 123.8, 121.6, 120.6, 119.9, 110.4, 109.8, 25.3, 20.9 ppm;

^{11}B NMR (128 MHz, C_6D_6) δ 1.4 ppm; HRMS (EI), calcd for $\text{C}_{36}\text{H}_{30}\text{BN}_3$ [M] $^+$: 515.2533, found 515.2518.

Synthesis of 5. Compound 5 was synthesized using a similar procedure as that for compound 1, where the second Grignard reagent was prepared with the low-temperature halogen-magnesium exchange described by Knochel (i.e., 1,3-bis(trifluoromethyl)-5-bromobenzene).¹⁷ 5 was obtained as a white powder in 8% yield (0.15 g). ^1H NMR (400 MHz, C_6D_6): δ 7.92 (d, J = 1.8 Hz, 2H, 3,5-bis CF_3 -Ph-H), 7.71 (s, 1H, 3,5-bis CF_3 -Ph-H), 7.53 (dd, J = 7.2, 1.4 Hz, 1H, Ph-H), 6.98 (td, J = 7.3, 1.1 Hz, 1H, Ph-H), 6.91 (td, J = 7.7, 1.3 Hz, 1H, Ph-H), 6.83 (s, 2H, Mes-H), 6.80 (d, J = 2.5 Hz, 1H, Pz-H), 6.62 (dd, J = 7.6, 1.6 Hz, 1H, Ph-H), 6.54 (t, J = 3.0 Hz, 1H, Pz-H), 5.46 (q, J = 2.5 Hz, 1H, Pz-H), 2.21 (s, 3H, *p*-Mes- CH_3), 1.72 (s, 6H, *o*-Mes- CH_3) ppm; ^{13}C NMR (100 MHz, C_6D_6) δ 142.3, 137.8, 135.8, 133.6, 132.2, 131.7, 131.4, 131.1, 130.8, 130.4, 127.5, 126.6, 126.1, 123.4, 122.1, 119.4, 110.6, 110.1, 25.5, 20.9 ppm; ^{11}B NMR (128 MHz, C_6D_6) δ 0.7 ppm; ^{19}F NMR (376 MHz, CD_2Cl_2) δ -63.04 (s, 6F, - CF_3) ppm; HRMS (EI), calcd for $\text{C}_{26}\text{H}_{21}\text{BN}_2\text{F}_6$ [M] $^+$: 486.1702, found 486.1717.

Synthesis of 6. Compound 6 was synthesized using the same procedure as that for compound 1, where 1-bromonaphthalene was used to prepare the second Grignard reagent in the synthesis of B(OMe)(Mes)(naphthalen-1-yl). 6 was obtained as a tan powder in 19% yield (0.19 g). ^1H NMR (400 MHz, C_6D_6): δ 8.72 (d, J = 8.4 Hz, 1H, naphthyl-H), 7.88 (d, J = 7.1 Hz, 1H, Ph-H), 7.74 (d, J = 8.1 Hz, 1H, naphthyl-H), 7.58 (d, J = 8.0 Hz, 1H, naphthyl-H), 7.50 (d, J = 2.4 Hz, 1H, Pz-H), 7.35–7.17 (m, 4H, naphthyl-H), 7.04 (t, J = 7.3 Hz, 1H, Ph-H), 6.99 (t, J = 7.5 Hz, 1H, Ph-H), 6.86 (s, 1H, Mes-H), 6.83 (s, 1H, Mes-H), 6.74 (d, J = 7.6 Hz, 1H), 6.66 (d, J = 2.6 Hz, 1H, Ph-H), 5.40 (d, J = 2.6 Hz, 1H, Pz-H), 2.23 (s, 3H, *o*-Mes- CH_3), 2.14 (s, 3H, *o*-Mes- CH_3), 1.69 (s, 3H, *p*-Mes- CH_3) ppm; ^{13}C NMR (100 MHz, C_6D_6) δ 177.3, 142.3, 140.5, 137.8, 137.0, 134.9, 134.8, 134.3, 132.8, 130.5, 129.4, 128.9, 126.8, 126.4, 126.0, 125.2, 124.9, 121.5, 110.3, 109.5, 26.5, 23.6, 21.0 ppm; ^{11}B NMR (128 MHz, C_6D_6) δ 2.4 ppm; HRMS (EI), calcd for $\text{C}_{28}\text{H}_{23}\text{BN}_2$ [M] $^+$: 400.2116, found 400.2110.

Synthesis of 7. In a 50 mL oven-dried Schlenk flask, mesityl magnesium bromide (35.1 mmol, 2.05 equiv) was prepared from 2-bromomesitylene (6.98 g, 35.1 mmol), magnesium turnings (0.86 g, 35.1 mmol), and a small iodine crystal in 30 mL of dry/degassed THF. The mixture was refluxed for 2 h at 80 °C until all the magnesium disappeared and then slowly cooled to 0 °C using an ice bath. After 30 min of cooling, the flask was charged with $\text{BF}_3\cdot\text{Et}_2\text{O}$ (~2.11 mL, 17.1 mmol, 1 equiv) and the solution was warmed to ambient temperature overnight. The solvent was removed *in vacuo* and the residue was extracted with dry/degassed hexanes (200 mL). The crude mixture was filtered through Celite under N_2 and concentrated under reduced pressure to afford B(F)Mes₂ as an off-white solid. A separate 50 mL Schlenk flask was charged with 1-(2-bromophenyl)-1H-pyrazole (0.38 g, 1.7 mmol) and 15 mL of dry/degassed Et_2O . The solution was cooled to -78 °C for 30 min, after which *n*-BuLi (0.72 mL, 1.8 mmol, 2.5 M in hexanes) was added dropwise. After stirring the lithiated ligand for 1 h at -78 °C, B(F)Mes₂ (0.53 g, 2.0 mmol, 1.2 equiv) was added to the flask and the mixture was allowed to stir overnight. The solvents were removed under reduced pressure and the crude product was purified with flash column chromatography using a gradient elution (10:1 → 4:1 hexanes: CH_2Cl_2). 7 was obtained as a pale-yellow powder in 69% yield (0.44 g). ^1H NMR (400 MHz, C_6D_6): δ 7.83 (d, J = 6.6 Hz, 1H, Ph-H), 7.37 (d, J = 2.2 Hz, 1H, Pz-H), 6.99–6.89 (m, 2H, Ph-H), 6.82 (s, 4H, Mes-H), 6.76–6.72 (m, 2H, Ph-H and Pz-H), 5.55 (d, J = 2.0 Hz, 1H, Pz-H), 2.21 (s, 6H, *p*-Mes- CH_3), 2.07 (s, 12H, *o*-Mes- CH_3) ppm; ^{13}C NMR (100 MHz, C_6D_6) δ 139.5, 136.8, 135.2, 134.1, 133.6, 130.3, 128.0, 127.8, 127.6, 127.4, 125.5, 121.2, 110.1, 109.7, 25.3, 21.0 ppm; ^{11}B NMR (128 MHz, C_6D_6) δ 2.2 ppm; HRMS (EI), calcd for $\text{C}_{27}\text{H}_{28}\text{BN}_2$ [M] $^+$: 392.2424, found 392.2421.

Photoisomerization Details. In a N_2 filled glovebox, 1–7 were added to J-Young NMR tubes to obtain concentrations of 10^{-2} M in C_6D_6 (~0.4 mL). The NMR tubes were sealed with their Teflon caps and removed from the glovebox. Photochemical experiments were

carried out using a Rayonet Photochemical Reactor (300 nm), and the photoisomerization processes of 1–7 were monitored periodically by ^1H , ^{11}B , and ^{19}F NMR (where applicable) until all compounds were converted to their diazaborepin isomers (1b–4b) or no additional spectral change was observed (5a–7a). The former were fully characterized by NMR, while the latter were identified based on their characteristic ^1H and ^{11}B resonances (see SI). Attempts to collect HRMS data of 1b–4b were unsuccessful due to their instability under air.

Data for 1b: ^1H NMR (400 MHz, C_6D_6): δ 8.01 (dd, J = 8.5, 1.4 Hz, 1H, Ph-H), 7.63 (d, J = 11.5 Hz, 1H, *p*-tolyl-H), 7.29–7.20 (m, 2H, Pz-H and Ph-H), 7.10 (d, J = 2.9 Hz, 1H, Pz-H), 6.93 (dd, J = 8.4, 1.3 Hz, 1H, Ph-H), 6.87 (s, 2H, Mes-H), 6.80 (ddd, J = 8.4, 6.9, 1.4 Hz, 1H, Ph-H), 6.35 (dd, J = 11.4, 1.1 Hz, 1H, *p*-tolyl-H), 5.55 (d, J = 5.3 Hz, 1H, *p*-tolyl-H), 5.48 (t, J = 2.9 Hz, 1H, Pz-H), 4.26 (d, J = 4.7 Hz, 1H, *p*-tolyl-H), 2.42 (s, 6H, *o*-Mes- CH_3), 2.21 (s, 3H, *p*-Mes- CH_3), 2.08 (s, 3H, *p*-tolyl- CH_3) ppm; ^{13}C NMR (100 MHz, C_6D_6) δ 141.2, 136.7, 134.2, 132.9, 132.1, 131.3, 129.9, 127.0, 126.6, 123.5, 123.5, 122.8, 120.4, 118.9, 114.9, 107.2, 33.5, 24.5, 21.4, 20.6 ppm; ^{11}B NMR (128 MHz, C_6D_6) δ 29.2 ppm.

Data for 2b: ^1H NMR (400 MHz, C_6D_6): δ 8.01 (d, J = 8.4 Hz, 1H, Ph-H), 7.63 (d, J = 11.5 Hz, 1H, B-Ph-H), 7.29–7.20 (m, 2H, Pz-H and Ph-H), 7.09 (d, J = 2.8 Hz, 1H, Pz-H), 6.93 (dd, J = 8.6, 1.3 Hz, 1H, Ph-H), 6.84 (s, 2H, Mes-H), 6.80 (ddd, J = 8.3, 6.7, 1.3 Hz, 1H, Ph-H), 6.36–6.32 (m, 1H, B-Ph-H), 6.23 (ddd, J = 10.7, 6.3, 1.8 Hz, 1H, B-Ph-H), 5.77 (dd, J = 10.6, 5.6 Hz, 1H, B-Ph-H), 5.48 (t, J = 2.9 Hz, 1H, Pz-H), 4.40 (dd, J = 5.7, 1.9 Hz, 1H, B-Ph-H), 2.45 (s, 6H, *o*-Mes- CH_3), 2.18 (s, 3H, *p*-Mes- CH_3) ppm; ^{13}C NMR (100 MHz, C_6D_6) δ 140.6, 136.7, 134.4, 133.1, 132.7, 130.9, 130.1, 129.2, 126.9, 126.4, 124.9, 124.7, 122.7, 119.9, 117.7, 115.2, 114.9, 107.2, 34.4, 21.2, 20.5 ppm; ^{11}B NMR (128 MHz, C_6D_6) δ 30.7 ppm.

Data for 3b: ^1H NMR (400 MHz, C_6D_6): δ 8.00 (dd, J = 8.4, 1.4 Hz, 1H, Ph-H), 7.29 (d, J = 3.0 Hz, 1H, Pz-H), 7.24 (m, 1H, Ph-H), 7.12 (d, J = 3.1 Hz, 1H, Pz-H), 6.95 (d, J = 8.6 Hz, 1H, Ph-H), 6.84 (s, 2H, Mes-H), 6.83–6.78 (m, 1H, Ph-H), 5.50 (t, J = 2.9 Hz, 1H, Pz-H), 2.46 (s, 6H, *o*-Mes- CH_3), 2.18 (s, 3H, *p*-Mes- CH_3) ppm; ^{13}C NMR (100 MHz, C_6D_6) δ 135.84, 134.48, 130.17, 129.10, 128.45, 128.33, 128.24, 128.05, 127.81, 127.57, 127.15, 127.07, 126.47, 124.82, 122.76, 120.31, 119.07, 115.08, 107.47, 21.22, 20.63 ppm; ^{11}B NMR (128 MHz, C_6D_6) δ 30.8 ppm.

Data for 4b: ^1H NMR (400 MHz, C_6D_6): δ 8.09 (d, J = 7.2 Hz, 2H, Cbz-H), 7.96 (m, 1H, Cbz-H), 7.94 (d, J = 8.8 Hz, 1H, Ph-H), 7.69 (d, J = 11.6 Hz, 1H, B-Ph-H), 7.65 (d, J = 8.0 Hz, 1H, Cbz-H), 7.30–7.20 (m, 6H, Cbz-H and Ph-H), 7.07 (d, J = 3.0 Hz, 1H, Pz-H), 6.93 (dd, J = 8.4, 1.0 Hz, 1H, Ph-H), 6.84 (m, 1H, Ph-H), 6.82 (s, 2H, Mes-H), 6.18 (dd, J = 11.6, 1.3 Hz, 1H, B-Ph-H), 6.13 (d, J = 6.3 Hz, 1H, B-Ph-H), 5.45 (t, J = 2.9 Hz, 1H, Pz-H), 4.41 (d, J = 6.3 Hz, 1H, B-Ph-H), 2.38 (bs, 6H, *o*-Mes- CH_3), 2.17 (s, 3H, *p*-Mes- CH_3) ppm; ^{13}C NMR (100 MHz, C_6D_6) δ 139.5, 137.8, 136.4, 135.5, 135.1, 132.5, 132.3, 130.6, 130.5, 128.8, 127.4, 127.0, 126.1, 125.8, 123.1, 121.4, 120.5, 120.0, 119.5, 119.3, 115.4, 111.0, 110.9, 107.9, 32.8, 21.5, 20.8 ppm; ^{11}B NMR (128 MHz, C_6D_6) δ 30.0 ppm.

X-ray Crystallographic Analysis. Colorless crystals of 4 and off-white crystals of 6 were grown by layering CH_2Cl_2 solutions of each with hexanes. The crystal data of compounds 4 and 6 were collected on a Bruker D8-Venture diffractometer with Mo $K\alpha$ radiation at 180 K. Data were processed using the Bruker APEX III software and SHELXTL software package (SHELXTL-2014/7)¹⁸ and corrected for absorption effects. All non-hydrogen atoms were refined anisotropically. The crystal data of 4 and 6 have been deposited at the Cambridge Crystallographic Data Center (CCDC Nos. 1858646 and 1858647).

■ ASSOCIATED CONTENT

● Supporting Information

The Supporting Information is available free of charge on the ACS Publications website at DOI: 10.1021/acs.organomet.8b00598.

Synthesis and characterization data, X-ray, TD-DFT calculation, and photoisomerization experiment data (PDF)

Cartesian coordinates for DFT optimized structures (XYZ)

Accession Codes

CCDC 1858646 and 1858647 contain the supplementary crystallographic data for this paper. These data can be obtained free of charge via www.ccdc.cam.ac.uk/data_request/cif, or by emailing data_request@ccdc.cam.ac.uk, or by contacting The Cambridge Crystallographic Data Centre, 12 Union Road, Cambridge CB2 1EZ, UK; fax: +44 1223 336033.

■ AUTHOR INFORMATION

Corresponding Author

*E-mail: wangs@chem.queensu.ca.

ORCID

Suning Wang: 0000-0003-0889-251X

Notes

The authors declare no competing financial interest.

■ ACKNOWLEDGMENTS

The authors thank the Natural Science and Engineering Research Council of Canada (RGPIN1193993-2013) for support.

■ REFERENCES

- (1) (a) Wakamiya, A. Incorporation of Boron into π -Conjugated Scaffolds to Produce Electron-Accepting π -Electron Systems. In *Main Group Strategies towards Functional Hybrid Materials*; Baumgartner, T., Jäkle, F., Eds.; John Wiley & Sons Ltd.: Hoboken, NJ, 2018; pp 1–22. (b) Liu, K.; Lalancette, A.; Jäkle, F. B–N Lewis Pair Functionalization of Anthracene: Structural Dynamics, Optoelectronic Properties, and O₂ Sensitization. *J. Am. Chem. Soc.* **2017**, *139*, 18170–18173. (c) Dou, C.; Saito, S.; Matsuo, K.; Hisaki, I.; Yamaguchi, S. A Boron-Containing PAH as a Substructure of Boron-Doped Graphene. *Angew. Chem., Int. Ed.* **2012**, *51*, 12206–12210. (d) Jäkle, F. Advances in the Synthesis of Organoborane Polymers for Optical, Electronic, and Sensory Applications. *Chem. Rev.* **2010**, *110*, 3985–4022. (e) Wakamiya, A.; Mori, K.; Yamaguchi, S. 3-Boryl-2,2'-bithiophene as a Versatile Core Skeleton for Full-Color Highly Emissive Organic Solids. *Angew. Chem., Int. Ed.* **2007**, *46*, 4273–4276.
- (2) (a) Chen, C.-H.; Gabbai, F. P. Exploring the Strong Hydrogen Bond Donor Properties of a Borinic Acid Functionality for Fluoride Anion Recognition. *Angew. Chem., Int. Ed.* **2018**, *57*, 521–525. (b) Wade, C. R.; Broomsgrove, A. E. J.; Aldridge, S.; Gabbai, F. P. Fluoride Ion Complexation and Sensing Using Organoboron Compounds. *Chem. Rev.* **2010**, *110*, 3958–3984. (c) Zhang, G.; Palmer, G. M.; Dewhirst, M. W.; Fraser, C. L. A Dual-Emissive-Materials Design Concept Enables Tumour Hypoxia Imaging. *Nat. Mater.* **2009**, *8*, 747–751. (d) Loudet, A.; Burgess, K. BODIPY Dyes and Their Derivatives: Syntheses and Spectroscopic Properties. *Chem. Rev.* **2007**, *107*, 4891–4932. (e) Yoshino, J.; Kano, N.; Kawashima, T. Fluorescence Properties of Simple N-Substituted Aldimines with a B–N Interaction and Their Fluorescence Quenching by a Cyanide Ion. *J. Org. Chem.* **2009**, *74*, 7496–7503. (f) Kano, N.; Yoshino, J.; Kawashima, T. Photoswitching of the Lewis Acidity of a Catecholborane Bearing an Azo Group Based on the Change in Coordination Number of Boron. *Org. Lett.* **2005**, *7*, 3909–3911.
- (3) (a) Wang, S.; Yang, D. T.; Lu, J. S.; Shimogawa, H.; Gong, S.; Wang, X.; Møllerup, S. K.; Wakamiya, A.; Chang, Y. L.; Yang, C.; Lu, Z. H. In Situ Solid-State Generation of (BN)₂-Pyrenes and Electroluminescent Devices. *Angew. Chem., Int. Ed.* **2015**, *54*, 15074–15078. (b) Li, D.; Zhang, H.; Wang, Y. Four-Coordinate Organoboron Compounds for Organic Light-Emitting Diodes (OLEDs). *Chem. Soc. Rev.* **2013**, *42*, 8416–8433. (d) Rao, Y.-L.; Wang, S. Four-Coordinate Organoboron Compounds with a π -Conjugated Chelate Ligand for Optoelectronic Applications. *Inorg. Chem.* **2011**, *50*, 12263–12274. (e) Liu, Q.-D.; Mudadu, M. S.; Thummel, R.; Tao, Y.; Wang, S. From Blue to Red: Syntheses, Structures, Electronic and Electroluminescent Properties of Tunable Luminescent N,N-Chelate Boron Complexes. *Adv. Funct. Mater.* **2005**, *15*, 143–154. (f) Chen, H.-Y.; Chi, Y.; Liu, C.-S.; Yu, J.-K.; Cheng, Y.-M.; Chen, K.-S.; Chou, P.-T.; Peng, S.-M.; Lee, G.-H.; Carty, A. J.; Yeh, S.-J.; Chen, C.-T. Rational Color Tuning and Luminescent Properties of Functionalized Boron-Containing 2-Pyridyl Pyrrolide Complexes. *Adv. Funct. Mater.* **2005**, *15*, 567–574.
- (4) (a) Kushida, T.; Shirai, S.; Ando, N.; Okamoto, T.; Ishii, H.; Matsui, H.; Yamagishi, M.; Uemura, T.; Tsurumi, J.; Watanabe, S.; Takeya, J.; Yamaguchi, S. Boron-Stabilized Planar Neutral π -Radicals with Well-Balanced Ambipolar Charge-Transport Properties. *J. Am. Chem. Soc.* **2017**, *139*, 14336–14339. (b) Poon, C.-T.; Wu, D.; Yam, V. W.-W. Boron(III)-Containing Donor-Acceptor Compound with Goldlike Reflective Behavior for Organic Resistive Memory Devices. *Angew. Chem., Int. Ed.* **2016**, *55*, 3647–3651. (c) Poon, C.-T.; Wu, D.; Lam, W. H.; Yam, V. W.-W. A Solution-Processable Donor–Acceptor Compound Containing Boron(III) Centers for Small-Molecule-Based High-Performance Ternary Electronic Memory Devices. *Angew. Chem., Int. Ed.* **2015**, *54*, 10569–10573. (d) Chang, Y.-L.; Rao, Y.-L.; Gong, S.; Ingram, G. L.; Wang, S.; Lu, Z.-H. Exciton-Stimulated Molecular Transformation in Organic Light-Emitting Diodes. *Adv. Mater.* **2014**, *26*, 6729–6733.
- (5) Rao, Y.-L.; Amarne, H.; Zhao, S.-B.; McCormick, T. M.; Martic, S.; Sun, Y.; Wang, R.-Y.; Wang, S. Reversible Intramolecular C–C Bond Formation/Breaking and Color Switching Mediated by a N,C-Chelate in (2-ph-py)BMes₂ and (5-BMes₂-2-ph-py)BMes₂. *J. Am. Chem. Soc.* **2008**, *130*, 12898–12900.
- (6) (a) Rao, Y.-L.; Hörl, C.; Braunschweig, H.; Wang, S. Reversible Photochemical and Thermal Isomerization of Azaboratabisnorcaradiene to Azaborabenzotropilidene. *Angew. Chem., Int. Ed.* **2014**, *53*, 9086–9089. (b) Rao, Y.-L.; Amarne, H.; Chen, L. D.; Brown, M. L.; Mosey, N. J.; Wang, S. Photo- and Thermal-Induced Multistructural Transformation of 2-Phenylazoly Chelate Boron Compounds. *J. Am. Chem. Soc.* **2013**, *135*, 3407–3410. (c) Rao, Y.-L.; Chen, L. D.; Mosey, N. J.; Wang, S. Stepwise Intramolecular Photoisomerization of NHC-Chelate Dimesitylboron Compounds with C–C Bond Formation and C–H Bond Insertion. *J. Am. Chem. Soc.* **2012**, *134*, 11026–11034.
- (7) (a) Møllerup, S. K.; Li, C.; Peng, T.; Wang, S. Regioselective Photoisomerization/C–C Bond Formation of Asymmetric B(ppy)-(Mes)(Ar): The Role of the Aryl Groups on Boron. *Angew. Chem., Int. Ed.* **2017**, *56*, 6093–6097. (b) Møllerup, S. K.; Li, C.; Radtke, J.; Wang, X.; Li, Q.-S.; Wang, S. Photochemical Generation of Chiral N,B,X-Heterocycles by Heteroaromatic C–X Bond Scission (X = S, O) and Boron Insertion. *Angew. Chem., Int. Ed.* **2018**, *57*, 9634–9639. (c) Møllerup, S. K.; Wang, S. Isomerization and Rearrangement of Boriranes: From Chemical Rarities to Functional Materials. *Sci. China Mater.* **2018**, *61*, 1249–1256.
- (8) Amarne, H.; Baik, C.; Murphy, S. K.; Wang, S. Steric and Electronic Influence on Photochromic Switching of N,C-Chelate Four-Coordinate Organoboron Compounds. *Chem. - Eur. J.* **2010**, *16*, 4750–4761.
- (9) Pappayee, N.; Mishra, A. K. Carbazole as an Excited State Proton Transfer Fluorescent Probe for Lipid Bilayers in Alkaline Medium. *Spectrochim. Acta, Part A* **2000**, *56*, 1027–1034.
- (10) (a) Paetzold, P.; Englert, U.; Finger, R.; Schmitz, T.; Tapper, A.; Ziembinski, R. Reactions at the Boron-Carbon Double Bond of Methyl(methylidene)boranes. *Z. Anorg. Allg. Chem.* **2004**, *630*, 508–

518. (b) Pilz, V. M.; Michel, H.; Berndt, A. Strong C–Sn Hyperconjugation in a Distannylmethyleneborane. *Angew. Chem., Int. Ed. Engl.* **1990**, *29*, 401–402. (c) Olmstead, M. M.; Power, P. P.; Weese, K. J.; Doedens, R. J. Isolation and X-ray Crystal Structure of the Boron Methylidenide Ion $[\text{Mes}_2\text{BCH}_2]^-$ (Mes = 2,4,6-Me₃C₆H₂): a Boron-Carbon Double Bonded Alkene Analog. *J. Am. Chem. Soc.* **1987**, *109*, 2541–2542.

(11) Hunold, R.; Pilz, M.; Allwohn, J.; Stadler, M.; Massa, W.; von Ragué Schleyer, P.; Berndt, A. Stable Methyleneboranes of High Lewis Acidity. *Angew. Chem., Int. Ed. Engl.* **1989**, *28*, 781–784.

(12) Das, A.; Ghosh, I.; König, B. Synthesis of Pyrrolo[1,2-*a*]quinolines and Ullazines by Visible Light Mediated One- and Twofold Annulation of N-Arylpyrroles with Arylalkynes. *Chem. Commun.* **2016**, *52*, 8695–8698.

(13) Wang, L.; Ji, E.; Liu, N.; Dai, B. Site-Selective N-Arylation of Carbazoles with Halogenated Fluorobenzenes. *Synthesis* **2016**, *48*, 737–750.

(14) Frisch, M. J.; Trucks, G. W.; Schlegel, H. B.; Scuseria, G. E.; Robb, M. A.; Cheeseman, J. R.; Scalmani, G.; Barone, V.; Mennucci, B.; Petersson, G. A.; Nakatsuji, H.; Caricato, M.; Li, X.; Hratchian, H. P.; Izmaylov, A. F.; Bloino, J.; Zheng, G.; Sonnenberg, J. L.; Hada, M.; Ehara, M.; Toyota, K.; Fukuda, R.; Hasegawa, J.; Ishida, M.; Nakajima, T.; Honda, Y.; Kitao, O.; Nakai, H.; Vreven, T.; Montgomery, J. A., Jr.; Peralta, J. E.; Ogliaro, F.; Bearpark, M.; Heyd, J. J.; Brothers, E.; Kudin, K. N.; Staroverov, V. N.; Keith, T. A.; Kobayashi, R.; Normand, J.; Raghavachari, K.; Rendell, A.; Burant, J. C.; Iyengar, S. S.; Tomasi, J.; Cossi, M.; Rega, N.; Millam, J. M.; Klene, M.; Knox, J. E.; Cross, J. B.; Bakken, V.; Adamo, C.; Jaramillo, J.; Gomperts, R.; Stratmann, R. E.; Yazyev, O.; Austin, A. J.; Cammi, R.; Pomelli, C.; Ochterski, J. W.; Martin, R. L.; Morokuma, K.; Zakrzewski, V. G.; Voth, G. A.; Salvador, P.; Dannenberg, J. J.; Dapprich, S.; Daniels, A. D.; Farkas, Ö.; Foresman, J. B.; Ortiz, J. V.; Cioslowski, J.; Fox, D. J. *Gaussian 09*, Revision C.01; Gaussian, Inc.: Wallingford, CT, 2010.

(15) (a) Lee, C.; Yang, W.; Parr, R. G. Development of the Colle-Salvetti Correlation-Energy Formula into a Functional of the Electron Density. *Phys. Rev. B: Condens. Matter Mater. Phys.* **1988**, *37*, 785–789. (b) Becke, A. D. A New Mixing of Hartree-Fock and Local Density-Functional Theories. *J. Chem. Phys.* **1993**, *98*, 1372–1377. (c) Becke, A. D. Density-Functional Theory Thermochemistry. III. The Role of Exact Exchange. *J. Chem. Phys.* **1993**, *98*, 5648–5652.

(16) (a) Schaefer, A.; Horn, H.; Ahlrichs, R. Fully Optimized Contracted Gaussian Basis Sets for Atoms Li to Kr. *J. Chem. Phys.* **1992**, *97*, 2571–2577. (b) Schaefer, A.; Huber, C.; Ahlrichs, R. Fully Optimized Contracted Gaussian Basis Sets of Triple Zeta Valence Quality for Atoms Li to Kr. *J. Chem. Phys.* **1994**, *100*, 5829–5835.

(17) Leazer, J. L.; Cvetovich, R.; Tsay, F.-R.; Dolling, U.; Vickery, T.; Bachert, D. An Improved Preparation of 3,5-Bis(trifluoromethyl)-acetophenone and Safety Considerations in the Preparation of 3,5-Bis(trifluoromethyl)phenyl Grignard Reagent. *J. Org. Chem.* **2003**, *68*, 3695–3698.

(18) *SHELXTL*, version 6.14; Bruker AXS: Madison, WI, 2000–2003.